

# Opportunities for Molecular Imaging in Multiple Sclerosis Management: Linking Probe to Treatment

Aline M. Thomas, PhD • Frederik Barkhof, MD, PhD • Jeff W. M. Bulte, PhD

From the Russell H. Morgan Department of Radiology and Radiological Science, Division of MR Research, the Johns Hopkins University School of Medicine, 733 N Broadway, Room 659, Baltimore, MD 21205 (A.M.T., J.W.M.B.); Cellular Imaging Section and Vascular Biology Program, Institute for Cell Engineering, the Johns Hopkins University School of Medicine, Baltimore, Md (A.M.T., J.W.M.B.); Department of Radiology and Nuclear Medicine, VU University Medical Center, Amsterdam, the Netherlands (F.B.); and Institutes of Neurology and Healthcare Engineering, University College London, London, England (F.B.). Received May 15, 2021; revision requested June 30; revision received January 11, 2022; accepted February 3. **Address correspondence to** J.W.M.B. (email: [jumbulte@mri.jhu.edu](mailto:jumbulte@mri.jhu.edu)).

J.W.M.B. is supported by a grant from the National Multiple Sclerosis Society (PP-1808-32367, RFA-2104-37460). A.M.T. is supported by a grant from the National Institutes of Health (K01EB030612). F.B. is supported by the National Institute of Health Research biomedical research center at University College London Hospitals.

Conflicts of interest are listed at the end of this article.

Radiology 2022; 303:486–497 • <https://doi.org/10.1148/radiol.211252> • Content codes: 

Imaging has been a critical component of multiple sclerosis (MS) management for nearly 40 years. The visual information derived from structural MRI, that is, signs of blood-brain barrier disruption, inflammation and demyelination, and brain and spinal cord atrophy, are the primary metrics used to evaluate therapeutic efficacy in MS. The development of targeted imaging probes has expanded our ability to evaluate and monitor MS and its therapies at the molecular level. Most molecular imaging probes evaluated for MS applications are small molecules initially developed for PET, nearly half of which are derived from U.S. Food and Drug Administration–approved drugs and those currently undergoing clinical trials. Superparamagnetic and fluorinated particles have been used for tracking circulating immune cells (in situ labeling) and immunosuppressive or remyelinating therapeutic stem cells (ex vivo labeling) clinically using proton (hydrogen 1 [ $^1\text{H}$ ]) and preclinically using fluorine 19 ( $^{19}\text{F}$ ) MRI. Translocator protein PET and  $^1\text{H}$  MR spectroscopy have been demonstrated to complement imaging metrics from structural (gadolinium-enhanced) MRI in nine and six trials for MS disease-modifying therapies, respectively. Still, despite multiple demonstrations of the utility of molecular imaging probes to evaluate the target location and to elucidate the mechanisms of disease-modifying therapies for MS applications, their use has been sparse in both preclinical and clinical settings.

© RSNA, 2022

**Online SA-CME** • See [www.rsna.org/learning-center-ry](http://www.rsna.org/learning-center-ry)

## Learning Objectives:

After reading the article and taking the test, the reader will be able to:

- State available biomarkers for profiling lesions and other forms of central nervous system damage in multiple sclerosis
- State clinically relevant modalities for molecular imaging biomarkers and their advantages and advances
- Explain the biochemical and pathologic relevance of molecular imaging biomarkers

## Accreditation and Designation Statement

The RSNA is accredited by the Accreditation Council for Continuing Medical Education (ACCME) to provide continuing medical education for physicians. The RSNA designates this journal-based SA-CME activity for a maximum of 1.0 AAMA PRA Category 1 Credit<sup>®</sup>. Physicians should claim only the credit commensurate with the extent of their participation in the activity.

## Disclosure Statement

The ACCME requires that the RSNA, as an accredited provider of CME, obtain signed disclosure statements from the authors, editors, and reviewers for this activity. For this journal-based CME activity, author disclosures are listed at the end of this article.

In multiple sclerosis (MS), abnormal activation of immune cells targeting myelin infiltrate, inflame, and damage the central nervous system (CNS), resulting in deficits that include cognitive and motor function. Imaging and histologic evidence have shown these events to have marked inter- and intraindividual variability (1–4). Treatment strategies have shifted over the years from nonspecific immunosuppressants to drugs that specifically target key molecules dysregulated in MS. With a continuously expanding number of targeted treatments for MS available and in development, there is a need for more specific imaging biomarkers. Current imaging metrics only partially capture these processes, and this limitation has encouraged the development and incorporation of molecular imaging biomarkers to improve image specificity and to monitor the mechanisms underlying effective therapies.

Herein, we describe the clinical utility of molecular imaging biomarkers for MS treatment evaluation to date and their potential use for new MS therapies that are in the developmental pipeline. We first briefly review the various modalities

used clinically for molecular imaging. Subsequently, within the pathophysiologic context of their molecular targets, we discuss probes that are currently in development alongside therapeutic drugs that share their targets. Emphasis is placed on how molecular imaging biomarkers can serve as surrogate end points in MS clinical trials and its animal model experimental allergic encephalomyelitis (EAE).

## Clinical Imaging Modalities

Proton MRI (hydrogen 1 [ $^1\text{H}$ ] MRI), MR spectroscopy (MRS), PET, and SPECT have been used for patients with MS since the early 1980s to evaluate structural and functional abnormalities in focal lesions and normal-appearing brain tissue. There is evidence of early attempts to image cellular targets (5), but successful molecular imaging of MS was only reported more recently. To date, MRI for treatment management of MS primarily relies on T1-weighted, T2-weighted, fluid-attenuated inversion recovery, and gadolinium-based contrast agent–enhanced sequences, which generate tissue and lesion contrast through differences in water content,

## Abbreviations

BBB = blood-brain barrier, CNS = central nervous system, EAE = experimental autoimmune encephalomyelitis, FDG = fluorodeoxyglucose, MPO = myeloperoxidase, MRS = MR spectroscopy, MS = multiple sclerosis, NAA = *N*-acetylaspartate, TSPO = translocator protein

## Summary

The authors present an update on PET and MRI molecular imaging biomarkers for diagnosing and treating multiple sclerosis and discuss their role in context of the severity of disease and their usefulness in evaluating response to existing treatments and those in the pipeline.

## Essentials

- Five of 12 current molecular imaging probes used in preclinical and clinical multiple sclerosis (MS) were adapted from U.S. Food and Drug Administration–approved MS therapies or those undergoing clinical trials.
- Four of six molecular imaging probes tested in patients with MS are visualized with PET.
- As of today, translocator protein PET has been used as a surrogate end point in 10 clinical trials for MS disease-modifying therapy.
- Hydrogen 1 MR spectroscopy has revealed alterations in *N*-acetylaspartate levels in five of six MS clinical trials for disease-modifying therapies.

proton relaxation, and blood brain barrier (BBB) integrity related to inflammation, demyelination, and neurodegeneration that are characteristic of MS. However, due to the higher specificity and sensitivity of imaging tracers, PET has recently gained more traction for molecular imaging of specific targets in MS.

## MRI and MRS

Although  $^1\text{H}$  MRI is widely used in patient care and clinical trials for patients with MS, its lack of molecular specificity limits its utility for understanding treatment mechanisms and efficacy. MRI sequences with higher pathologic specificity in the assessment of neurodegeneration and demyelination, such as diffusion tensor, magnetization transfer, and magnetic susceptibility–weighted imaging, are increasingly used as outcome measures in clinical trials (6). Sodium 23 ( $^{23}\text{Na}$ ) (7,8) and phosphorus 31 ( $^{31}\text{P}$ ) (9) MRI and MRS have been evaluated in patients with MS to quantify sodium content and protein phosphorylation, respectively. Recently translated amide proton transfer (10,11) and inhomogeneous magnetization transfer (12,13) MRI have been able to depict alterations in lesions and “normal appearing” white matter of patients with MS that cannot be observed using T2- and T2\*-weighted MRI. The incorporation of contrast agents expanded the pathophysiologic processes that can be visualized for MS treatment management, particularly those associated with acute focal lesions. Gadolinium-based contrast agents are routinely used to detect BBB disruption. In situ cell labeling using iron oxide particles has been used to monitor immune cell trafficking and/or infiltration (14). Preclinically, fluorine 19 ( $^{19}\text{F}$ )–containing nano-emulsions have also been explored as a more specific alternative to iron for immune cell tracking (15).

$^1\text{H}$  MRS has revealed changes in brain levels of creatine and *N*-acetylaspartate (NAA) in preclinical models (16) and clinically in patients with MS (17), although this technique has lower spatial resolution than structural MRI and lower chemical sensitivity than

PET.  $^1\text{H}$  MRS has been used as a secondary end point for several clinical trials in patients with MS (see “ $^1\text{H}$  MRS” under “Clinical Trial End Points”). The NAA level is associated with the presence of neurons as a marker of axonal integrity and is often normalized to the creatine level, which is considered a marker of total cell presence (18). However, monitoring transport and metabolism requires the use of tracers whose flux can be monitored. With further development of hyperpolarization, a technique that enhances the detection of probes with nonproton nuclei (eg, carbon 13 [ $^{13}\text{C}$ ] and xenon 129) in MRS imaging, chemical sensitivity can be enhanced to levels that permit monitoring altered use of metabolic pathways (eg, glycolysis). Although lactate production has successfully been imaged and quantified using hyperpolarized  $^{13}\text{C}$  pyruvate in humans (19), this imaging technique requires specialized equipment only available in a few clinical centers.

## PET and SPECT

The high sensitivity of radioisotopes for the detection of specific targets with PET and SPECT not only permits the visualization of rare low-expressed markers, but also has been used to evaluate transport limitations, for example through the BBB, retention time, and target specificity of existing and candidate drugs (20). However, these modalities require ionizing radiation and usually must be paired with CT or MRI for anatomic reference. Recent advances include time-of-flight PET, which can enhance temporal resolution (21), the point-spread function, which can improve spatial resolution (22), and depth of interaction detector, which has been used to enable total body imaging in humans (23).

Multiple PET tracers have been developed on the basis of  $^{11}\text{C}$  (half-life of 20 minutes), gallium 68 ( $^{68}\text{Ga}$ ) (half-life of 68 minutes), fluorine 18 ( $^{18}\text{F}$ ) (half-life of 110 minutes), copper 64 ( $^{64}\text{Cu}$ ) (half-life of 13 hours), and zirconium 89 (half-life of 3.3 days) (24), with a wide range of molecular targets from naturally occurring metabolites to antibodies to small molecules. The evaluation of multiple biomarkers may prove beneficial in treatment selection, but because all PET tracers emit equivalent rays, sequential administration of imaging of probes would be needed. Kinetic models are typically required to accurately quantify tracer uptake, further complicating the use of this modality for imaging multiple biomarkers. Despite poorer resolution and sensitivity, the advantage of SPECT is that gamma rays are detected, the energy of which is specific to the tracer, permitting the simultaneous visualization of multiple probes (25,26) or the combined imaging of SPECT probes with a PET probe (27). Still, this modality has been sparsely explored for applications in patients with MS (28,29).

## Biomarkers of MS Targets

As many of these biomarkers reflect the targets or pathways of approved MS therapies or those currently in development, they have the potential to assist in treatment selection. Small molecule probes that have been tested in patients with MS can help monitor aspects of disease pathophysiology ranging from glial activation (30) and demyelination (31) to neurodegeneration (32). Even more probes, including nanoparticles and cell-labeling agents, have been evaluated in preclinical models for monitoring other aspects of MS progression. Still, few probes and biomarkers in-

| Molecular Imaging Biomarkers Used to Evaluate Disease-modifying Therapies for MS |                                    |          |                           |                  |                           |              |               |  |
|--|------------------------------------|----------|---------------------------|------------------|---------------------------|--------------|---------------|--|
| Molecular Target/Cell Type   | Imaging Label                      | Modality | Evaluation or Application |                  |                           |              |               | Ligand Name                                  |
|  |                                    |          | Animal Models             | Patients with MS | Clinical Trial End Points | Other Probes |               |  |
| NA/immune  | <sup>19</sup> F, USPIO             | MRI      | Yes                       | Yes              | Yes                       | No           | No            | NA   |
| NA/transplanted  | <sup>19</sup> F, USPIO             | MRI      | Yes                       | Yes              | Yes                       | No           | No            | NA   |
| CD20/immune  | <sup>64</sup> Cu, <sup>89</sup> Zr | PET      | Yes                       | Yes              | No                        | No           | No            | Rituximab                                    |
| COX-2/immune   | <sup>11</sup> C                    | PET      | No                        | No               | No                        | No           | No            | Celecoxib                                    |
| Dihydro-orotate dehydrogenase/immune   | <sup>19</sup> F                    | MRI      | Yes                       | No               | No                        | No           | No            | Teriflunomide                                |
| GABA A receptors/neuron  | <sup>11</sup> C                    | PET      | No                        | Yes              | Yes                       | No           | No            | Flumazenil                                   |
| GLUT1/multiple   | <sup>18</sup> F                    | PET      | Yes                       | Yes              | Yes                       | No           | PK-11195, ... | FDG  |
| ICAM-1/endothelial   | GBCA, MPIO                         | MRI      | Yes                       | No               | No                        | No           | No            | NA   |
| Metabolites/multiple   | <sup>1</sup> H                     | MRS      | Yes                       | Yes              | Yes                       | Yes          | No            | NA   |
| Myeloperoxidase/immune   | GBCA                               | MRI      | Yes                       | No               | No                        | No           | No            | AZD5904, AZD3421                             |
| Potassium channels/neuron  | <sup>18</sup> F                    | PET      | N                         | No               | Yes                       | No           | No            | 4-AP   |
| Serotonin receptors/neuron   | <sup>11</sup> C                    | PET      | Yes                       | Yes              | No                        | No           | No            | Clozapine                                    |
| Translocator protein/microglia   | <sup>11</sup> C, <sup>18</sup> F   | PET      | Yes                       | Yes              | Yes                       | Yes          | FDG           | DPA-713, GE-180, PBR06, PBR28, PK-11195, ... |
| VCAM-1/endothelial cell  | GBCA, MPIO                         | MRI      | Yes                       | No               | No                        | No           | No            | NA   |

Note.—4-AP = 4-aminopyridine, <sup>11</sup>C = carbon 11, COX-2 = cyclooxygenase-2, <sup>64</sup>Cu = copper 64, FDG = fluorodeoxyglucose, <sup>18</sup>F = fluorine 18, <sup>19</sup>F = fluorine 19, GABA A =  $\gamma$ -aminobutyric acid type A, GBCA = gadolinium-based contrast agent, GLUT1 = glucose transporter 1, <sup>1</sup>H = hydrogen 1, ICAM-1 = intracellular adhesion molecule type 1, MPIO = micron-sized particles of iron oxide, MRS = MR spectroscopy, MS = multiple sclerosis, NA = not applicable, USPIO = ultrasmall superparamagnetic iron oxide, <sup>89</sup>Zr = zirconium 89.

investigated for applications in patients with MS have been assessed for evaluating treatment efficacy. Probes that have been developed and evaluated for MS treatment management are primarily (candidate) MS drugs and therapies repurposed for imaging applications (Table).

### Small Molecule Probes and Nanoparticles

The unique advantages in probe sensitivity, specificity, and resolution have encouraged the development of multimodal scanners and multimodal imaging probes to overcome current imaging limitations and expand the number of molecular targets and variety of probes that can be imaged clinically. Although not yet applied to MS, advancements have been made in nanotechnology, particularly for PET/MRI. At the present time, imaging probes are available clinically to monitor most CNS cell types; however, they have yet to be explored for MS applications. Differences among animal species (eg, BBB permeability) remain an obstacle for developing and translating targeted molecular imaging probes for MS applications, as exemplified

by the limited PET signal of 2-chloro-2'-deoxy-2'-fluoro-9- $\beta$ -D-arabinofuranosyl-adenine (33) in the human brain.

Intracellular and vascular cellular adhesion molecule type 1 (intracellular adhesion molecule type 1 [ICAM-1] and vascular adhesion molecule type 1), endothelial surface markers that enable leukocyte infiltration, are expressed at a higher level in patients with MS (34) and have been imaged preclinically using antibodies conjugated to MRI- or US-visible nanoparticles. Antibodies rarely can be used across species, but a monoclonal antibody targeting ICAM-1 (enlimomab) has been developed and tested in humans for other applications (35). ICAM-1 detection in EAE rats decreased over threefold on US images upon administration of methylprednisolone treatment (36). Gadolinium-loaded liposomes (37) and micron-sized particles of iron oxide (38) developed for MRI of ICAM-1 and vascular adhesion molecule type 1 have been tested in rodent MS models. Because MRI suffers from low sensitivity compared with PET, nanoparticles or liposomes that can be doped with multiple imaging probes to amplify signal are advantageous for target-specific imaging of endothelial cells, as

these probes do not need to cross the BBB.

Myeloperoxidase (MPO) is a lysosomal hemoprotein that is secreted by activated leukocytes and microglia. Its presence and activity are higher in demyelinating MS lesions (39), and the presence of the G/G variant is linked to faster rates of disease progression (40). Chen et al (41) used bis-5-hydroxytryptamide-diethylenetriamine-pentaacetate (bis-HT-DTPA) attached to gadolinium (bis-HT-DTPA-Gd) as an MPO-activatable paramagnetic sensor for imaging its activity in EAE. bis-HT-DTPA-Gd oligomerizes in the presence of the radicals generated by MPO, shortening the T1 to enhance detection. With use of the same imaging approach, a twofold decrease in MPO enzymatic activity was seen on 4-aminobenzoic hydrazide administration (Fig 1) (42). In murine MS models, the inhibitors ABAH (4-aminobenzoic hydrazide) and KYC (*N*-acetyl lysyltyrosylcysteine amide) both attenuated paralysis in part through tissue sparing (43). The MPO inhibitors AZD5904 and AZD3421 have been tested in humans for other applications (44).

Glucose uptake and metabolism have been investigated preclinically for lesion detection and profiling using  $^{18}\text{F}$  fluorodeoxyglucose (FDG) PET and hyperpolarized pyruvate (MRS imaging), respectively (45,46). Although glucose use is not an active target of MS therapies, both fumarate (47) and interferon- $\beta$  (48) are associated with alterations in glucose utilization. FDG uptake occurs through glucose transporter 1 (GLUT1), the primary transporter for glucose, and, therefore, can be used to quantify its activity. Enhanced GLUT1 expression has been observed in MS lesions compared with normal-appearing tissues (49). Clinically, FDG uptake has been used to evaluate cognitive (50) and physical (51) impairments. Preclinically, increased FDG uptake was detected in lesions of EAE rats and signal intensity correlated

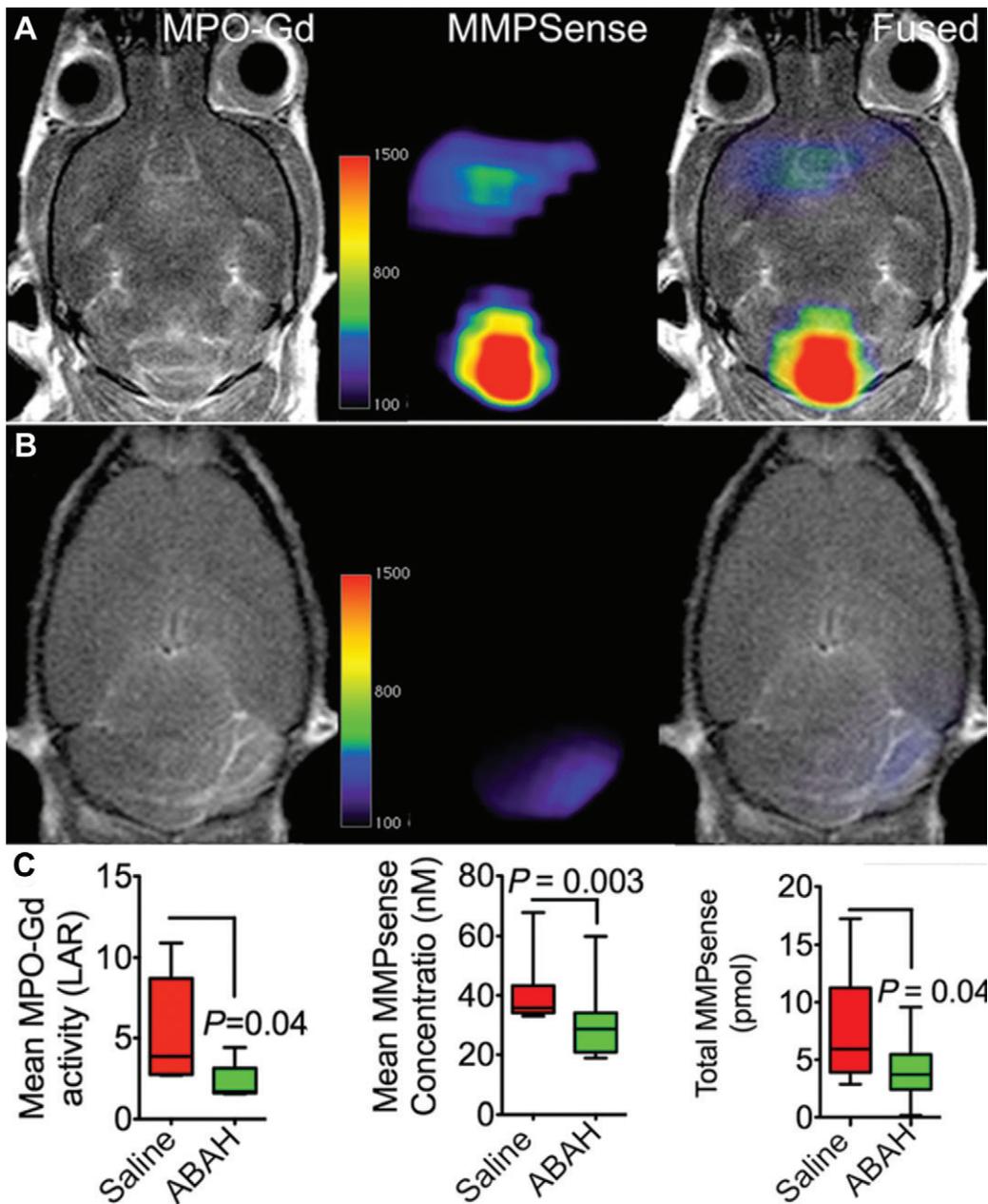


**Figure 1:** Imaging myeloperoxidase (MPO) activity after administration of its inhibitor 4-aminobenzoic hydrazide (ABAH) in a mouse multiple sclerosis model. (A, B) T1-weighted MRI and fluorescent scans after injection of bis-5-hydroxytryptamide-diethylenetriamine-pentaacetate (MPO-Gd) and MMPsense-680 (Perkin-Elmer). (C) Box-and-whisker plots show signal quantification upon injection of saline with and without administration of the MPO inhibitor. LAR = lesion activation ratio. (Adapted, with permission, from reference 42.)

significantly with immune cell infiltration (45). The opposite was observed in a cuprizone mouse model (52), which may be a reflection of the more extensive cell loss characteristic of this model. Still, administration of caspase-1 inhibitor VX-765 restored FDG uptake in cuprizone mice to normal levels.

Unlike most of the other imaging probes discussed in this review, FDG has been compared with several human-tested probes with potential for use in MS treatment management. Uptake in lesions was more consistently higher with FDG than with fluorothymidine, a probe used to monitor nucleoside uptake, and fluoro-ethyl-tyrosine, an imaging biomarker for amino acid uptake (45). Uptake of the latter two probes was only observed in some

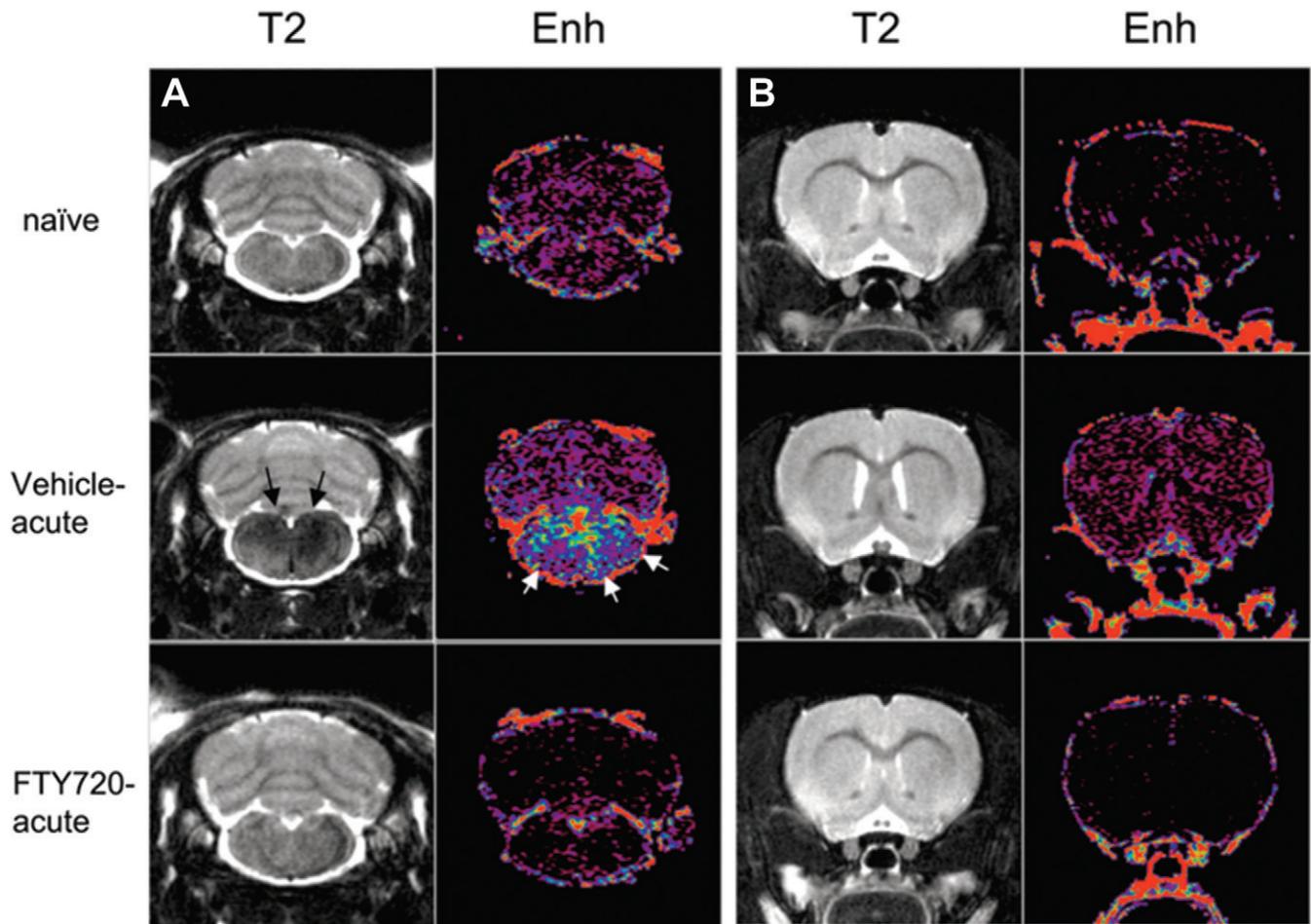


**Figure 2:** T2-weighted images of immune cell infiltration after fingolimod treatment in a rat multiple sclerosis model. T2-weighted MRI scans of (A) medulla and cerebellum and (B) cortex and striatum after intravenous injection of ultrasmall superparamagnetic iron oxide particles. Imaging was performed to monitor inflammatory macrophages in rats. Ultrasmall superparamagnetic iron oxide-enhanced images reveal decreases in macrophage brain infiltration after administration of the s1p antagonist FTY720 (fingolimod) compared to control (injection vehicle only), including in brain regions without apparent low signal intensity. Enh = enhanced. (Adapted, under a CC BY license, from reference 62.)

lesions *ex vivo* (autoradiography). Their limited uptake may be a reflection of more inflamed regions during the acute stages of lesion development or may be due to an inability to cross the BBB as observed with 2-chloro-2'-deoxy-2'-fluoro-9- $\beta$ -D-arabinofuranosyl-adenine, another nucleoside probe (33). In another study (53), FDG uptake was related to PK-11195, a probe for translocator protein, and S-4-(3-fluoropropyl)-L-glutamic acid (FSPG), a probe for glutamate and/or cysteine antiporter activity; however, only FSPG could monitor disease activity in a rat MS model.

#### In Situ-labeled Cells

Imaging of endogenous monocyte and/or macrophage activity and trafficking may be a sensitive biomarker for early detection of MS lesions. These cells are among the most numerous cells found in CNS lesions in human MS and in EAE models (54). They are represented by both resident macrophages and infiltrating monocytes, with the latter believed to play the most prominent role in driving disease pathogenesis (55). Monocyte depletion before symptom development leads to delays in EAE onset and reduction in severity of symptoms, whereas depletion after onset shows reduced disease progression (56). It has been shown in preclinical models (57,58) and patients with MS (14,59,60) that early lesions

can be identified with *in situ* labeling by systemic injection of ultrasmall superparamagnetic iron oxide particles (61). This imaging approach, which labels circulating immune cells, particularly monocyte and/or macrophages, was used for preclinical evaluation of FTY720 (fingolimod) (Fig 2) (62), which inhibits the egression of T cells from reactive lymph nodes. Upon FTY720 administration, ultrasmall superparamagnetic iron oxide enhancement (rendering lesions hypointense on T2-weighted images) was dramatically reduced in the cerebellum. Because FTY720 is an s1p receptor antagonist, that study demonstrates how imaging can help guide the development of new therapeutic regimens.

Like ultrasmall superparamagnetic iron oxide particles, intravenously injected fluorinated emulsions known as perfluorocarbons can also be taken up by mononuclear phagocytic cells. As the naturally abundant  $^{19}\text{F}$  isotope can generate a signal on MRI scans similar to that of protons when tuned to the corresponding resonance frequency (63), it is possible to visualize fluorine "hot spots" on MRI scans. One of the earliest studies on uptake of perfluorocarbon-labeled macrophages in EAE by Nöth et al (64) demonstrated signal in the vertebral bodies adjacent to the cervical spinal cord rather than the spinal tissue itself, suggesting that macrophages egressed from these sites toward CNS inflammation.

Interestingly, later studies observed similar uptake in bone marrow cavities in the vicinity of spinal cord lesions, which was reduced following administration of cyclophosphamide (Fig 3) (65).

### Imaging Agents Based on Established Therapeutic Drugs

Nearly half of the imaging probes that have been explored for MS applications are based on drugs that are U.S. Food and Drug Administration–approved for or clinically tested in patients with MS. As targets of pathophysiologic processes that are observed in MS, these imaging probes have potential utility as surrogate end points in clinical trials. Yet, except for dalfampridine (66), establishing their biodistribution has been the primary objective of reports to date that radiolabeled these drugs for MS imaging applications.

Serotonin is a neurotransmitter whose uptake, expression, and transmission is altered in MS (67). Lower levels ( $\leq 100$  ng/ $10^9$  platelets) of circulating serotonin correspond with fatigue severity score ( $P = .046$ ) and depression (Beck scale,  $P = .024$ ) in MS (68). Although the role of serotonin in MS progression is not well understood, it does appear to modulate  $\gamma$ -aminobutyric acid-ergic and glutamatergic transmission (69). Clozapine (70) and risperidone (71) are serotonin (and dopamine) receptor antagonists with anti-inflammatory properties that have been shown to attenuate disease severity in EAE. Clozapine and risperidone were tested in patients with MS (CRISP, or Community ReIntegration for Socially isolated Patients, trial, ACTRN12616000178448), but the trial was halted early due to a higher incidence of adverse side effects during the titration stage (72), prompting investigations into the pharmacodynamics of these drugs. Robichon et al (73) investigated the biodistribution of clozapine in a mouse EAE model using matrix-assisted laser desorption ionization, or MALDI, imaging (73). Higher levels (fivefold) of clozapine in the serum were observed in EAE mice compared with control mice. Higher levels (threefold) of its metabolite, norclozapine, were also observed in the serum of EAE mice.  $^{11}\text{C}$ -labeled clozapine imaging in healthy humans revealed 7.6% uptake in the brain (74). However, further investigations are needed to determine if the higher metabolism of these drugs observed in EAE caused the adverse effects in the CRISP trial (71).

Celecoxib, a clinical cyclooxygenase-2 (COX-2) inhibitor that was shown to attenuate a murine model of MS (75), has also been converted into a PET probe ( $^{11}\text{C}$ ). To our knowledge it has not yet been evaluated for applications in patients with MS, but uptake was reported in multiple brain regions of healthy baboons (76). COX-2, also known as prostaglandin-endoperoxide synthase type 2, is an intracellular enzyme expressed by activated microglia and immune cells that has also been suggested as an MS biomarker. The enzyme is upregulated in MS lesions (77). Its most widely developed inhibitor, aspirin, alleviated fatigue in 10 of 26 patients with MS (38.5%) (78) and has also attenuated paralysis in multiple MS models (79).

Dalfampridine, also known as 4-aminopyridine, is a potassium channel blocker approved for patients with MS. On myelinated neurons,  $\text{Kv}_{1.1-1.4}$  channels release potassium into the extracellular space to repolarize their axons to their unstimulated, pre-axon potential state. Preclinically, 4-aminopyridine has been shown to attenuate paralysis in a mouse MS model (80). Clinically, this drug has been shown to improve both cognitive and motor functions in

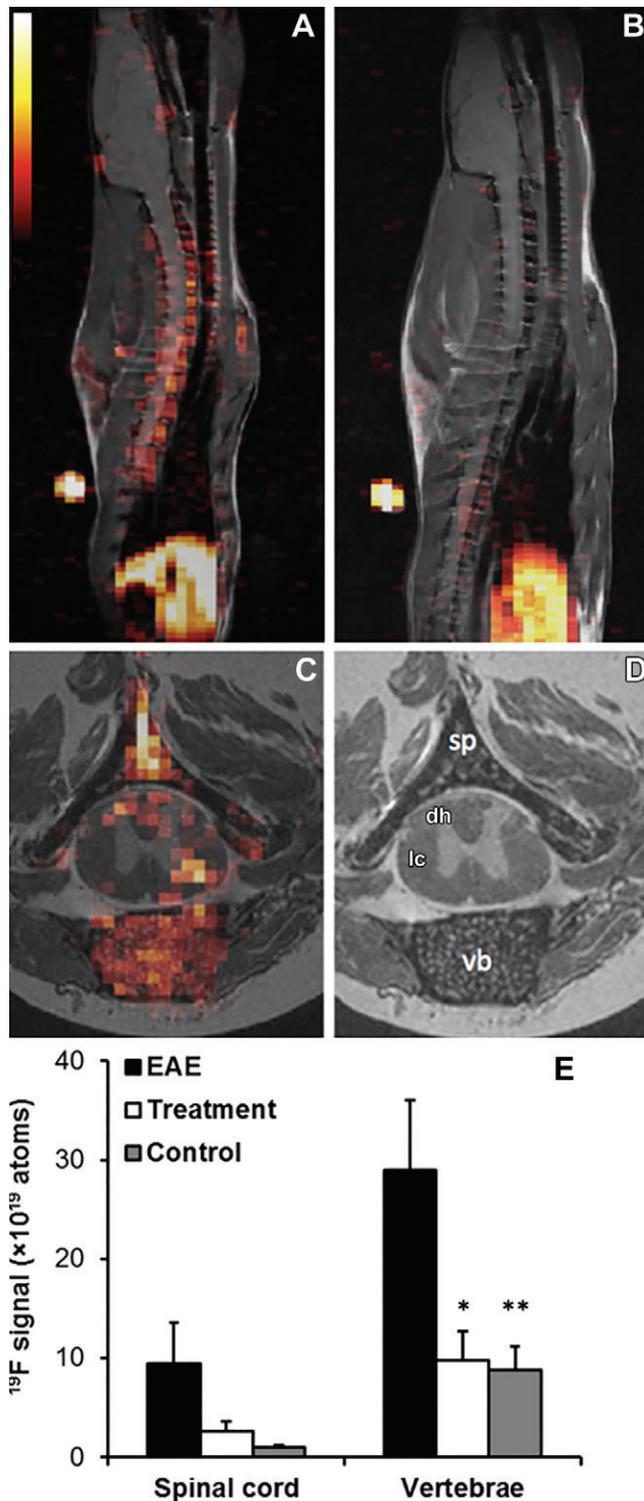


**Figure 3:** Fluorine 19 ( $^{19}\text{F}$ ) imaging of immune infiltration after cyclophosphamide treatment in a rat multiple sclerosis model. (A–D)  $^{19}\text{F}$  MRI scans of inflammatory macrophages in (A, C) an experimental autoimmune encephalomyelitis rat and (B, D) a normal control rat following systemic perfluorocarbon injection show accumulation of injected perfluorocarbon outside the central nervous system in adjacent peri-spinal bone marrow cavities. dh = dorsal horn, lc = lateral column, sp = spine, vb = vertebral body. (Adapted, under a CC BY license, from reference 65.) (E) Bar graph shows quantification of infiltrates after prophylactic injection of an antineoplastic treatment, cyclophosphamide. \* =  $P < .05$  for EAE versus treatment, \*\* =  $P < .05$  for EAE versus control. EAE = experimental autoimmune encephalomyelitis. (Adapted, under a CC BY license, from reference 65.)

patients with MS (81,82). A fluorinated version of the drug was developed by Brugarolas et al (66) for PET imaging. Probe uptake on autoradiographs corresponded to dysmyelinated regions in the shiverer mouse model and demyelinated regions in a diphtheria toxin-A genetic mouse model, as confirmed with histologic examination. In a rat lysolethicin MS model, probe uptake was observed in the lysolethicin-injected group in the corpus callosum. In healthy rhesus monkeys, probe uptake was observed in all brain regions, demonstrating its ability to cross the BBB, but well below saturation levels, as would be expected in absence of injury (66).

Flumazenil is a  $\gamma$ -aminobutyric acid type A receptor antagonist clinically used to treat benzodiazepine toxicity. Receptors of the inhibitory neurotransmitter are present in neurons and to some extent in immune cells, and its activity is dysregulated in MS (83). Flumazenil has already been developed into a PET tracer and evaluated in patients with MS as an imaging biomarker for disease progression (Fig 4) (32). Flumazenil uptake in gray matter was 10% lower in patients with MS compared with healthy controls and correlated well with lesion load at T2-weighted MRI, suggesting its utility as a marker of neurodegeneration. More recently, flumazenil uptake was compared with  $^{11}\text{C}$ -PK11195 (translocator protein) uptake (84). In that study, the overall cortical uptake of the two tracers showed positive correlation with each other; however, when the cortex was segmented, correlation was not observed in all regions. The therapeutic benefits of flumazenil have not been explored for MS applications, but valproate and phenobarbitone were shown to reduce paralysis in a rat EAE model (85) and diazepam decreased immune cell infiltration in a similar model (86).

Rituximab is a B cell–targeting antibody used by patients with MS off-label (87). James et al (88) incorporated  $^{64}\text{Cu}$  to visualize the drug using PET. With use of transgenic mice that express humanized CD20, enhanced uptake was observed in the MS model at locations of B220-positive B cell presence. In contrast to the copper-labeled probe in the mouse model, a zirconium-labeled version of rituximab could not penetrate the CNS in humans (89). The differences in BBB permeability between the two species highlight another potential hurdle for translating antibody-based therapies and imaging probes. Other anti-CD20 antibodies, specifically ocrelizumab, ofatumumab, and ublituximab, have successfully undergone phase II clinical trials for MS (90–92).

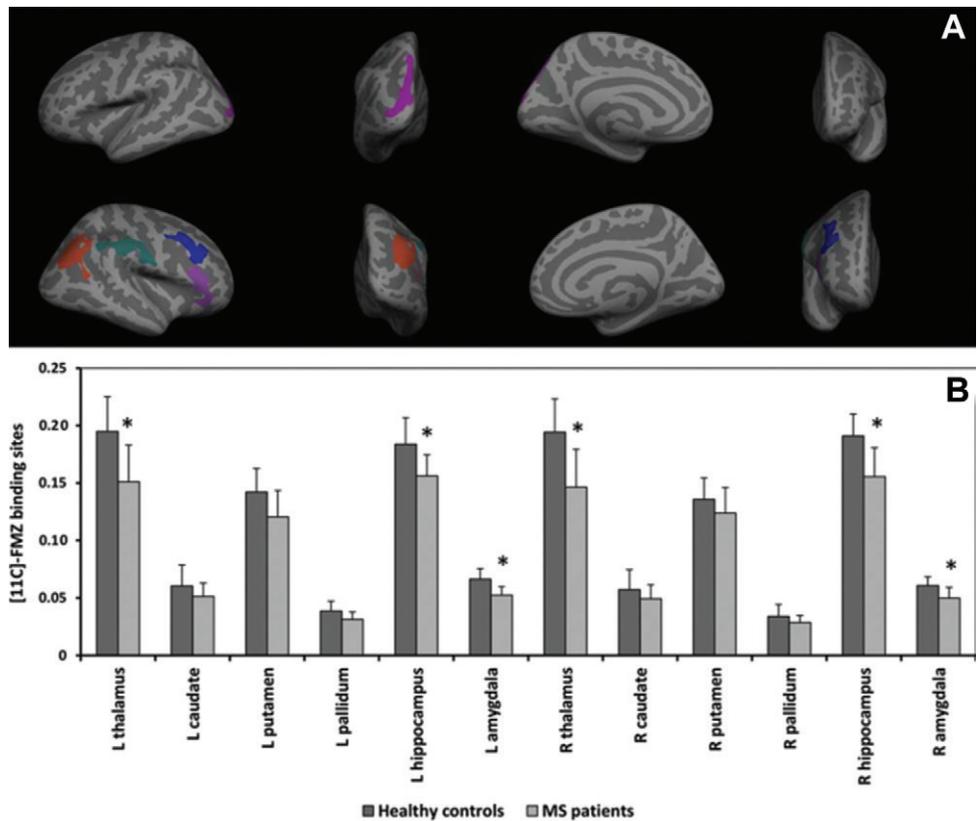


**Figure 4:** Uptake of the multiple sclerosis (MS) drug flumazenil (FMZ) in patients. **(A)** Flumazenil PET ( $^{11}\text{C}$ ) images reveal regions with lower uptake in patients with MS after correction for age and sex. **(A)** Visualization and **(B)** quantification of these regions in the left (upper row in **A**) and right (lower row in **A**) hemispheres. \* =  $P < .05$  between hemispheres. (Adapted, with permission, from reference 32.)

Recently,  $^{64}\text{Cu}$ -labeled anti-CD19 monoclonal antibodies were used to visualize B-cell trafficking in EAE mice (93).

Teriflunomide is an approved MS treatment that inhibits the dihydro-orotate dehydrogenase enzyme used during cell division (94), which is hypothesized to slow the proliferation of activated immune cells. The drug contains three fluorines, which when substituted with  $^{19}\text{F}$  can be imaged using  $^{19}\text{F}$  MRS. Prinz et al (95) characterized the responsiveness and biodistribution of this drug in the SJL/J relapse-remitting and C57Bl/6 progressive EAE mouse models. Through ex vivo images (autoradiography) they showed less cerebrospinal fluid and brain uptake in the C57Bl/6 EAE mice, which were nonresponsive, compared with healthy mice and SJL/J EAE mice, which were drug responsive. They detected additional peaks when teriflunomide was administered, but not in teriflunomide solution. They hypothesized these additional peaks were teriflunomide metabolites, which are of clinical interest given their long retention time (15 days).

In vivo cell tracking of transplanted therapeutic cells using contrast agents or cellular reporter genes may be used to determine their spatiotemporal fate. Exogenous neural stem and/or neural progenitor cells and mesenchymal stem and/or stromal cells have been administered in EAE rodents and patients with MS to induce remyelination and immunosuppression, respectively. At the time of this writing (January 2022), there are 12 active clinical trials registered with ClinicalTrials.gov on the use of mesenchymal stem cells in patients with MS. On injection, it is believed that these

cells are homing into inflammatory lesions resulting from migration-stimulating cytokine cues, but systemic immunosuppression in lymph nodes has also been suggested (96). One approach is MRI tracking of cells labeled ex vivo with superparamagnetic iron oxide before administration, a currently used clinical approach (97). Indeed, superparamagnetic iron oxide-labeled cells could be tracked in rat (98) and mouse (99,100) EAE models and, when injected systematically, were found to localize in the spinal cord and around occipital horns of patients with MS (101).

### Clinical Trial End Points

Despite the multitude of molecular imaging biomarkers clinically tested and approved, conventional imaging metrics, particularly gadolinium enhancement, new and/or enlarging T2-hyperintense lesions, and brain atrophy, remain the commonly used imaging parameters to evaluate therapeutic efficacy in MS clinical trials (6).  $^1\text{H}$  MRS of endogenous metabolites and translocator protein (TSPO) PET have both been used as surrogate end points in several trials of approved MS drugs. Both imaging biomarkers revealed progression independently of or differentially to conventional imaging metrics, demonstrating the potential for novel molecular imaging metrics as secondary end points for drugs under development.

### $^1\text{H}$ MRS

$^1\text{H}$  MRS is by far the most extensively characterized and used MRS technique for monitoring metabolic changes in the brain. Such alterations are associated with nearly every aspect of MS pathophysiology—including immune activation, excitotoxicity, and cellular degeneration. Seven classes of U.S. Food and Drug Administration–approved MS therapies are linked to metabolic pathways. Fumarate (47) and interferon- $\beta$  (48) alter glycolytic enzymes. Fingolimod and mitoxantrone target key players in glycolysis (102,103) and glutaminolysis (102,104). Cladribine (105) and teriflunomide (94) alter enzymes responsible for nucleotide metabolism.

$^1\text{H}$  MRS has been a component of multiple MS clinical trials as a secondary imaging end point for evaluating therapeutic

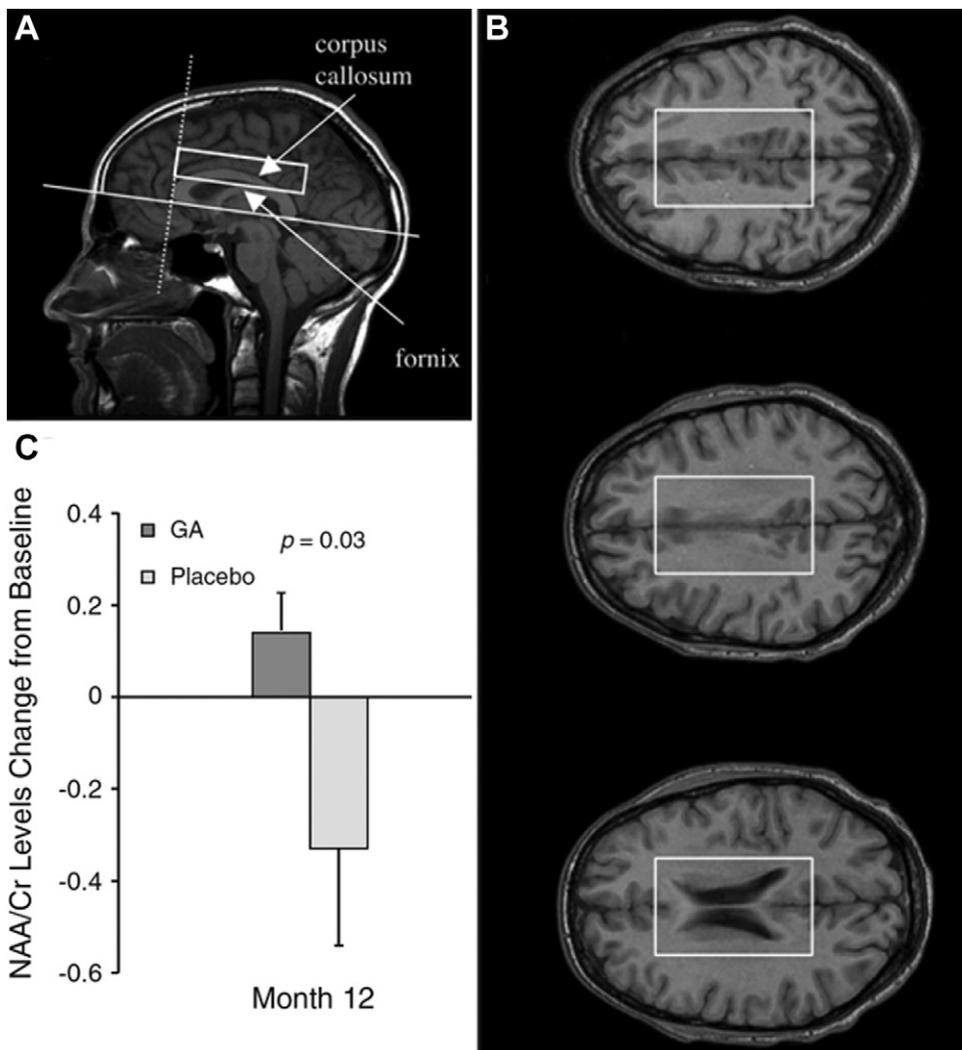


**Figure 5:** Use of hydrogen 1 ( $^1\text{H}$ ) MR spectroscopy (MRS) as a surrogate end point in multiple sclerosis (MS) clinical trials. Images illustrate the changes in the ratio of N-acetylaspartate (NAA) to creatine in patients with MS after receiving glatiramer acetate (GA) or placebo. (A, B) Images from  $^1\text{H}$  MRS illustrate voxel regions that were analyzed. (Adapted, under a CC BY license, from reference 17.) (C) Bar graph shows quantification of the NAA-to-creatine (Cr) ratio after 12 months of treatment. (Adapted, under a CC BY license, from reference 17.)

efficacy. Interferon- $\beta$  therapy was shown to increase creatine and choline levels (106). Patients receiving glatiramer acetate in PreCISE, or the Prospective Randomized trial of the optimal Evaluation of Cardiac Symptoms and revascularization, had higher ratios of NAA to creatine than those who received placebo (17) (Fig 5). NAA, choline, creatine, inositol, lactate, glutamine, and glutamate levels did not change upon receiving natalizumab (107). Changes in phosphate and NAA levels after receiving fumarate are being monitored (ClinicalTrials.gov identifier: NCT02644083, results not yet available online). The ratio of NAA to creatine increased over time after ocrelizumab treatment (90). Notably, monitoring the NAA-to-creatine ratio using  $^1\text{H}$  MRS outperformed lesion assessment as a predictor of future disability in patients with MS receiving glatiramer acetate in a 20-year longitudinal study (108). In a preclinical MS model, NAA content in teriflunomide-treated mice correlated significantly ( $P < .05$ ) with the presence of CC1-positive oligodendrocytes (109).

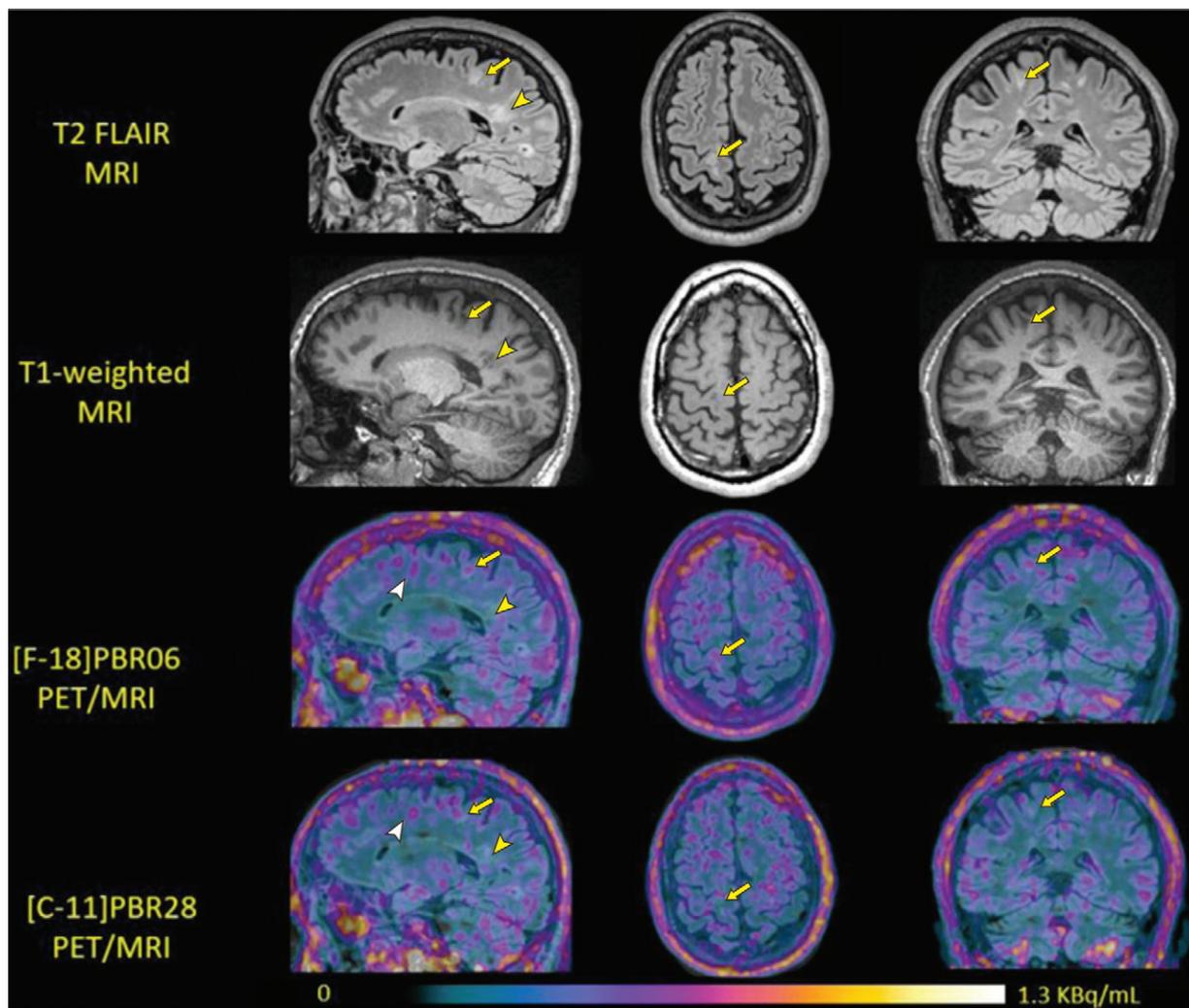


**Figure 6:** Images illustrate comparison of two probes targeting translocator protein (TSPO), a microglial activation biomarker, in patients with multiple sclerosis. Yellow arrows and arrowheads highlight the positions of lesions identified on T1-weighted images. White arrowheads indicate a lesion only identified with PET/MRI. The uptake of PBR-06 and PBR-28 did not necessarily correspond with these lesions or each other.  $^{11}\text{C}$  = carbon 11,  $^{18}\text{F}$  = fluorine 19, FLAIR = fluid-attenuated inversion recovery. (Adapted, with permission, from reference 113.)

### TSPO Imaging

TSPO was first targeted in patients with MS more than 20 years ago using the PET probe ( $^{11}\text{C}$ )-PK-11195 (30). TSPO, previously known as peripheral benzodiazepine receptor, is a mitochondrial protein involved in steroid metabolism. The upregulated expression of TSPO in the brain is associated with activated microglia and reactive astrocytes and, to a lesser extent, activated macrophages. The PBR28 tracer developed later had 1.2-fold to twofold higher uptake in binders (those with  $>60\%$  brain signal at 13 minutes compared with peak signal, indicating probe retention) compared with ( $^{11}\text{C}$ )-PK-11195 when both were injected into the same volunteers (110), although PK-11195 had 1.3- to 1.8-fold higher uptake in nonbinders (those with a  $<60\%$  ratio). Recently, TSPO distribution was compared in patients with relapsing-remitting and progressive MS using PBR28 (111). A 1.3- to 1.5-fold higher TSPO uptake was observed in focal lesions for both patient samples compared with brain cortex in healthy volunteers.

Currently, more than 10 TSPO-targeting probes with  $^{18}\text{F}$  or  $^{11}\text{C}$  as the radiolabel have been evaluated in humans (112)

and many more are in development, arguably making TSPO the most extensively developed molecular imaging target. The variability in binding strength and location of these second-generation probes can be used to differentiate TSPO variants to visualize their inter- and inpatient heterogeneity in expression. Still, few studies have compared these probes side-by-side in vivo for applications in MS (110,113,114) (Fig 6). In rodent EAE models, antagonists etifoxine and, to a lesser extent, emapunil (XBD173) decreased paralysis and spinal cord inflammation (115). Currently, patients are being recruited to evaluate changes in TSPO at administration of these anxiolytic drugs in patients with MS (ClinicalTrials.gov identifier: NCT03850301).

Recently, TSPO PET has been used as a secondary imaging end point for 10 clinical trials of MS disease-modifying therapies ([clinicaltrials.gov/ct2/results?cond = Multiple+Sclerosis&term = tspo](https://clinicaltrials.gov/ct2/results?cond=Multiple+Sclerosis&term=tspo)). TSPO PET has been evaluated in clinical trials of interferon- $\beta$  using tracer DPA-713 (116), glatiramer acetate using PBR06 (117), natalizumab using PK-11195 (118), and ATB-555 using PBR-28 (ClinicalTrials.gov identifier: NCT02606630).

DPA-713 (116) and PK-11195 (119) have also been used in clinical trials of fingolimod. DPA-713 is so far the only tracer that has been used for side-by-side comparison of treatments (116). Unlike the others, this study revealed enhanced neuroinflammation in several treated patients who were clinically and radiologically stable. PK-11195 uptake transiently increased in the absence of gadolinium-based contrast agent-enhancing lesions (119). Ongoing clinical trials use PBR06 for alemtuzumab (ClinicalTrials.gov identifier: NCT03983252), PBR28 for ocrelizumab (ClinicalTrials.gov identifier: NCT04230174), and PK-11195 for cladribine (ClinicalTrials.gov identifier: NCT04239820). Preclinically, GE-180 has also been tested for fingolimod and natalizumab (120). Surprisingly, there has been little consensus in tracer choice both clinically and preclinically for treatment evaluation using TSPO imaging. Furthermore, none of the drugs evaluated in patients with MS and MS models share molecular targets with TSPO.

## Conclusion

During the past 30 years, molecular imaging has been increasingly used in multiple sclerosis (MS) for elucidating therapeutic mechanisms and monitoring treatment outcomes in clinical trials. The clinical success of  $^1\text{H}$  MR spectroscopy (108) in outperforming gadolinium-enhanced imaging for predicting future disability and of translocator protein PET imaging (111) to complement structural MRI metrics in detecting disease-induced brain alterations has opened the door for the development, translation, and application of molecular imaging biomarkers for MS. Although molecular imaging biomarkers are primarily being used to better understand therapeutic mechanisms, they also have the potential to assist in treatment decisions in patients with MS. We highlighted numerous examples of probes and drugs tested and/or translated for MS applications with shared molecular targets that can be used similarly. In the near future, imaging these biomarkers for managing treatment in patients with MS may provide an opportunity to individualize treatment from the array of existing therapeutic drugs and help determine eligibility in clinical trials for new candidate drugs.

**Disclosures of conflicts of interest:** A.M.T. No relevant relationships. F.B. Member of the *Radiology* editorial board. J.W.M.B. Member of the *Radiology* editorial board; paid board member at NovaDip Biosciences, SuperBranche, and NanomediGene; paid medical-legal consultant for expert testimony; grants/grants pending to institution; payment for lectures including service on speakers bureaus; patents (planned, pending, or issued); royalties for books; travel/accommodations/meeting expenses unrelated to activities listed.

## References

- Faizy TD, Thaler C, Kumar D, et al. Heterogeneity of Multiple Sclerosis Lesions in Multislice Myelin Water Imaging. *PLoS One* 2016;11(3):e0151496.
- Tham M, Frischer JM, Weigand SD, et al. Iron Heterogeneity in Early Active Multiple Sclerosis Lesions. *Ann Neurol* 2021;89(3):498–510.
- Yao B, Ikonomidou VN, Cantor FK, Ohayon JM, Duyn J, Bagnato F. Heterogeneity of Multiple Sclerosis White Matter Lesions Detected With T2\*-Weighted Imaging at 7.0 Tesla. *J Neuroimaging* 2015;25(5):799–806.
- Eisele P, Konstantin S, Griebel M, et al. Heterogeneity of acute multiple sclerosis lesions on sodium ( $^{23}\text{Na}$ ) MRI. *Mult Scler* 2016;22(8):1040–1047.
- Herscovitch P, Dischino DD, Kilbourn MR, Welch MJ, Raichle ME. Myelin imaging with C-11 labeled diphenylmethanol and positron emission tomography. *J Nucl Med* 1985;26(5):104. [https://inis.iaea.org/search/search.aspx?orig\\_q=RN:18060757](https://inis.iaea.org/search/search.aspx?orig_q=RN:18060757).
- Tur C, Moccia M, Barkhof F, et al. Assessing treatment outcomes in multiple sclerosis trials and in the clinical setting. *Nat Rev Neurol* 2018;14(2):75–93.
- Zaaraoui W, Konstantin S, Audoin B, et al. Distribution of brain sodium accumulation correlates with disability in multiple sclerosis: a cross-sectional  $^{23}\text{Na}$  MR imaging study. *Radiology* 2012;264(3):859–867.
- Petracca M, Vancea RO, Fleysher L, Jonkmann LE, Oesingmann N, Inglese M. Brain intra- and extracellular sodium concentration in multiple sclerosis: a 7 T MRI study. *Brain* 2016;139(Pt 3):795–806.
- Hattinger E, Magerkurth J, Pilatus U, Hübers A, Wahl M, Ziemann U. Combined (1)H and (31)P spectroscopy provides new insights into the pathobiochemistry of brain damage in multiple sclerosis. *NMR Biomed* 2011;24(5):536–546.
- By S, Barry RL, Smith AK, et al. Amide proton transfer CEST of the cervical spinal cord in multiple sclerosis patients at 3T. *Magn Reson Med* 2018;79(2):806–814.
- Sartoretti E, Sartoretti T, Wyss M, et al. Amide Proton Transfer Weighted Imaging Shows Differences in Multiple Sclerosis Lesions and White Matter Hyperintensities of Presumed Vascular Origin. *Front Neurol* 2019;10:1307.
- Rasoanandrianina H, Demortière S, Trabelsi A, et al. Sensitivity of the Inhomogeneous Magnetization Transfer Imaging Technique to Spinal Cord Damage in Multiple Sclerosis. *AJNR Am J Neuroradiol* 2020;41(5):929–937.
- Zhang L, Wen B, Chen T, et al. A comparison study of inhomogeneous magnetization transfer (ihMT) and magnetization transfer (MT) in multiple sclerosis based on whole brain acquisition at 3.0 T. *Magn Reson Imaging* 2020;70:43–49.
- Douset V, Brochet B, Deloire MS, et al. MR imaging of relapsing multiple sclerosis patients using ultra-small-particle iron oxide and compared with gadolinium. *AJNR Am J Neuroradiol* 2006;27(5):1000–1005.
- Waiczies S, Millward JM, Starke L, et al. Enhanced Fluorine-19 MRI Sensitivity using a Cryogenic Radiofrequency Probe: Technical Developments and Ex Vivo Demonstration in a Mouse Model of Neuroinflammation. *Sci Rep* 2017;7(1):9808.
- Lee DW, Kwon JI, Woo CW, et al. In Vivo Measurement of Neurochemical Abnormalities in the Hippocampus in a Rat Model of Cuprizone-Induced Demyelination. *Diagnostics (Basel)* 2020;11(1):E45.
- Arnold DL, Narayanan S, Antel S. Neuroprotection with glatiramer acetate: evidence from the PreCISE trial. *J Neurol* 2013;260(7):1901–1906.
- Narayana PA. Magnetic resonance spectroscopy in the monitoring of multiple sclerosis. *J Neuroimaging* 2005;15(4 Suppl):46S–57S.
- Miloushev VZ, Granlund KL, Boltyanskiy R, et al. Metabolic Imaging of the Human Brain with Hyperpolarized  $^{13}\text{C}$  Pyruvate Demonstrates  $^{13}\text{C}$  Lactate Production in Brain Tumor Patients. *Cancer Res* 2018;78(14):3755–3760.
- Mathews PM, Rabiner EA, Paschier J, Gunn RN. Positron emission tomography molecular imaging for drug development. *Br J Clin Pharmacol* 2012;73(2):175–186.
- Conti M. Focus on time-of-flight PET: the benefits of improved time resolution. *Eur J Nucl Med Mol Imaging* 2011;38(6):1147–1157.
- Akamatsu G, Ishikawa K, Mitsumoto K, et al. Improvement in PET/CT image quality with a combination of point-spread function and time-of-flight in relation to reconstruction parameters. *J Nucl Med* 2012;53(11):1716–1722.
- Berg E, Roncali E, Kapusta M, Du J, Cherry SR. A combined time-of-flight and depth-of-interaction detector for total-body positron emission tomography. *Med Phys* 2016;43(2):939–950.
- Coenen HH, Erment J. Expanding PET-applications in life sciences with positron-emitters beyond fluorine-18. *Nucl Med Biol* 2021;92:241–269.
- Guo Z, Gao M, Zhang D, et al. Simultaneous SPECT imaging of multi-targets to assist in identifying hepatic lesions. *Sci Rep* 2016;6(1):28812.
- Hapdey S, Soret M, Buvat I. Quantification in simultaneous (99m)Tc/(123)I brain SPECT using generalized spectral factor analysis: a Monte Carlo study. *Phys Med Biol* 2006;51(23):6157–6171.
- Blower JE, Bordoloi JK, Rigby A, et al. Protocols for Dual Tracer PET/SPECT Preclinical Imaging. *Front Phys* 2020;8(126):126.
- Lorberboym M, Lampl Y, Nikolov G, Sadeh M, Gilad R. I-123 MIBG cardiac scintigraphy and autonomic test evaluation in multiple sclerosis patients. *J Neurol* 2008;255(2):211–216.
- Mattner F, Katsifis A, Staykova M, Ballantyne P, Willenborg DO. Evaluation of a radiolabelled peripheral benzodiazepine receptor ligand in the central nervous system inflammation of experimental autoimmune encephalomyelitis: a possible probe for imaging multiple sclerosis. *Eur J Nucl Med Mol Imaging* 2005;32(5):557–563.
- Vowinckel E, Reutens D, Becher B, et al. PK11195 binding to the peripheral benzodiazepine receptor as a marker of microglia activation in multiple sclerosis and experimental autoimmune encephalomyelitis. *J Neurosci Res* 1997;50(2):345–353.
- Bodini B, Veronese M, García-Lorenzo D, et al. Dynamic Imaging of Individual Remyelination Profiles in Multiple Sclerosis. *Ann Neurol* 2016;79(5):726–738.

32. Freeman L, Garcia-Lorenzo D, Bottin L, et al. The neuronal component of gray matter damage in multiple sclerosis: A [(11) C]flumazenil positron emission tomography study. *Ann Neurol* 2015;78(4):554–567.
33. Chen BY, Ghezzi C, Villegas B, et al. <sup>18</sup>F-FAC PET Visualizes Brain-Infiltrating Leukocytes in a Mouse Model of Multiple Sclerosis. *J Nucl Med* 2020;61(5):757–763.
34. Washington R, Burton J, Todd RF 3rd, Newman W, Dragovic L, Dore-Duffy P. Expression of immunologically relevant endothelial cell activation antigens on isolated central nervous system microvessels from patients with multiple sclerosis. *Ann Neurol* 1994;35(1):89–97.
35. Mileski WJ, Burkhart D, Hunt JL, et al. Clinical effects of inhibiting leukocyte adhesion with monoclonal antibody to intercellular adhesion molecule-1 (enlimomab) in the treatment of partial-thickness burn injury. *J Trauma* 2003;54(5):950–958.
36. Reinhardt M, Hauff P, Linker RA, et al. Ultrasound derived imaging and quantification of cell adhesion molecules in experimental autoimmune encephalomyelitis (EAE) by Sensitive Particle Acoustic Quantification (SPAQ). *Neuroimage* 2005;27(2):267–278.
37. Sipskins DA, Gijbels K, Tropper FD, Bednarski M, Li KC, Steinman L. ICAM-1 expression in autoimmune encephalitis visualized using magnetic resonance imaging. *J Neuroimmunol* 2000;104(1):1–9.
38. Serres S, Mardiguian S, Campbell SJ, et al. VCAM-1-targeted magnetic resonance imaging reveals subclinical disease in a mouse model of multiple sclerosis. *FASEB J* 2011;25(12):4415–4422.
39. Gray E, Thomas TL, Betmouni S, Scolding N, Love S. Elevated activity and microglial expression of myeloperoxidase in demyelinated cerebral cortex in multiple sclerosis. *Brain Pathol* 2008;18(1):86–95.
40. Zakrzewska-Pniewska B, Styczynska M, Podlecka A, et al. Association of apolipoprotein E and myeloperoxidase genotypes to clinical course of familial and sporadic multiple sclerosis. *Mult Scler* 2004;10(3):266–271.
41. Chen JW, Breckwoldt MO, Aikawa E, Chiang G, Weissleder R. Myeloperoxidase-targeted imaging of active inflammatory lesions in murine experimental autoimmune encephalomyelitis. *Brain* 2008;131(Pt 4):1123–1133.
42. Zhang Y, Dong H, Seeburg DP, et al. Multimodal Molecular Imaging Demonstrates Myeloperoxidase Regulation of Matrix Metalloproteinase Activity in Neuroinflammation. *Mol Neurobiol* 2019;56(2):954–962.
43. Yu G, Zheng S, Zhang H. Inhibition of myeloperoxidase by N-acetyl l-cysteine amide reduces experimental autoimmune encephalomyelitis-induced injury and promotes oligodendrocyte regeneration and neurogenesis in a murine model of progressive multiple sclerosis. *Neuroreport* 2018;29(3):208–213.
44. Galijasevic S. The development of myeloperoxidase inhibitors. *Bioorg Med Chem Lett* 2019;29(1):1–7.
45. Buck D, Förschler A, Lapa C, et al. 18F-FDG PET detects inflammatory infiltrates in spinal cord experimental autoimmune encephalomyelitis lesions. *J Nucl Med* 2012;53(8):1269–1276.
46. Guglielmetti C, Najac C, Didonna A, Van der Linden A, Ronen SM, Chauveil MM. Hyperpolarized <sup>13</sup>C MR metabolic imaging can detect neuroinflammation in vivo in a multiple sclerosis murine model. *Proc Natl Acad Sci U S A* 2017;114(33):E6982–E6991.
47. Kornberg MD, Bhargava P, Kim PM, et al. Dimethyl fumarate targets GAPDH and aerobic glycolysis to modulate immunity. *Science* 2018;360(6387):449–453.
48. La Rocca C, Carbone F, De Rosa V, et al. Immunometabolic profiling of T cells from patients with relapsing-remitting multiple sclerosis reveals an impairment in glycolysis and mitochondrial respiration. *Metabolism* 2017;77:39–46.
49. Nijland PG, Michailidou I, Witte ME, et al. Cellular distribution of glucose and monocarboxylate transporters in human brain white matter and multiple sclerosis lesions. *Glia* 2014;62(7):1125–1141.
50. Paulesu E, Perani D, Fazio F, et al. Functional basis of memory impairment in multiple sclerosis: a [18F]FDG PET study. *Neuroimage* 1996;4(2):87–96.
51. Rudroff T, Kindred JH, Koo PJ, Karki R, Hebert JR. Asymmetric glucose uptake in leg muscles of patients with Multiple Sclerosis during walking detected by [18F]-FDG PET/CT. *NeuroRehabilitation* 2014;35(4):813–823.
52. Saito LB, Fernandes JB, Smith MJ, et al. Intranasal anti-caspase-1 therapy preserves myelin and glucose metabolism in a model of progressive multiple sclerosis. *Glia* 2021;69(1):216–229.
53. Martín A, Vázquez-Villoldo N, Gómez-Vallejo V, et al. In vivo imaging of system xc<sup>-</sup> as a novel approach to monitor multiple sclerosis. *Eur J Nucl Med Mol Imaging* 2016;43(6):1124–1138.
54. Brück W, Sommermeier N, Bergmann M, et al. Macrophages in multiple sclerosis. *Immunobiology* 1996;195(4-5):588–600.
55. Nally FK, De Santi C, McCoy CE. Nanomodulation of Macrophages in Multiple Sclerosis. *Cells* 2019;8(6):543.
56. Brosnan CF, Bornstein MB, Bloom BR. The effects of macrophage depletion on the clinical and pathologic expression of experimental allergic encephalomyelitis. *J Immunol* 1981;126(2):614–620.
57. Xu S, Jordan EK, Brocke S, et al. Study of relapsing remitting experimental allergic encephalomyelitis SJL mouse model using MION-46L enhanced in vivo MRI: early histopathological correlation. *J Neurosci Res* 1998;52(5):549–558.
58. Dousset V, Delalande C, Ballarino L, et al. In vivo macrophage activity imaging in the central nervous system detected by magnetic resonance. *Magn Reson Med* 1999;41(2):329–333.
59. Vellinga MM, Oude Engberink RD, Seewann A, et al. Pluriformity of inflammation in multiple sclerosis shown by ultra-small iron oxide particle enhancement. *Brain* 2008;131(Pt 3):800–807.
60. Vellinga MM, Vrenken H, Hulst HE, et al. Use of ultrasmall superparamagnetic particles of iron oxide (USPIO)-enhanced MRI to demonstrate diffuse inflammation in the normal-appearing white matter (NAWM) of multiple sclerosis (MS) patients: an exploratory study. *J Magn Reson Imaging* 2009;29(4):774–779.
61. Bulte JW, Frank JA. Imaging macrophage activity in the brain by using ultrasmall particles of iron oxide. *AJNR Am J Neuroradiol* 2000;21(9):1767–1768.
62. Rausch M, Hiestand P, Foster CA, Baumann DR, Cannet C, Rudin M. Predictability of FTY720 efficacy in experimental autoimmune encephalomyelitis by in vivo macrophage tracking: clinical implications for ultrasmall superparamagnetic iron oxide-enhanced magnetic resonance imaging. *J Magn Reson Imaging* 2004;20(1):16–24.
63. Ruiz-Cabello J, Barnett BP, Bottomley PA, Bulte JW. Fluorine (19F) MRS and MRI in biomedicine. *NMR Biomed* 2011;24(2):114–129.
64. Nöth U, Morrissey SP, Deichmann R, et al. Perfluoro-15-crown-5-ether labelled macrophages in adoptive transfer experimental allergic encephalomyelitis. *Artif Cells Blood Substit Immobil Biotechnol* 1997;25(3):243–254.
65. Zhong J, Narsinh K, Morel PA, Xu H, Ahrens ET. In Vivo Quantification of Inflammation in Experimental Autoimmune Encephalomyelitis Rats Using Fluorine-19 Magnetic Resonance Imaging Reveals Immune Cell Recruitment outside the Nervous System. *PLoS One* 2015;10(10):e0140238.
66. Brugarolas P, Sánchez-Rodríguez JE, Tsai HM, et al. Development of a PET radioligand for potassium channels to image CNS demyelination. *Sci Rep* 2018;8(1):607.
67. Hesse S, Moeller F, Petroff D, et al. Altered serotonin transporter availability in patients with multiple sclerosis. *Eur J Nucl Med Mol Imaging* 2014;41(5):827–835 [Published correction appears in *Eur J Nucl Med Mol Imaging* 2014;41(8):1640–1641].
68. Baidina TV, Akintseva YV, Trushnikova TN. Platelet serotonin in multiple sclerosis and its relationship with fatigue syndrome. *Neurochem J* 2013;7(3):226–229.
69. Ciranna L. Serotonin as a modulator of glutamate- and GABA-mediated neurotransmission: implications in physiological functions and in pathology. *Curr Neuropharmacol* 2006;4(2):101–114.
70. Green LK, Zareie P, Templeton N, Keyzers RA, Connor B, La Flamme AC. Enhanced disease reduction using clozapine, an atypical antipsychotic agent, and glatiramer acetate combination therapy in experimental autoimmune encephalomyelitis. *Mult Scler J Exp Transl Clin* 2017;3(1):205217317698724.
71. O'Sullivan D, Green L, Stone S, et al. Treatment with the antipsychotic agent, risperidone, reduces disease severity in experimental autoimmune encephalomyelitis. *PLoS One* 2014;9(8):e104430.
72. La Flamme AC, Abernethy D, Sim D, et al. Safety and acceptability of clozapine and risperidone in progressive multiple sclerosis: a phase I, randomised, blinded, placebo-controlled trial. *BMJ Neurol Open* 2020;2(1):e000060.
73. Robichon K, Sondhauss S, Jordan TW, Keyzers RA, Connor B, La Flamme AC. Localisation of clozapine during experimental autoimmune encephalomyelitis and its impact on dopamine and its receptors. *Sci Rep* 2021;11(1):2966.
74. Park HS, Kim E, Moon BS, Lim NH, Lee BC, Kim SE. In Vivo Tissue Pharmacokinetics of Carbon-11-Labeled Clozapine in Healthy Volunteers: A Positron Emission Tomography Study. *CPT Pharmacometrics Syst Pharmacol* 2015;4(5):305–311.
75. Miyamoto K, Miyake S, Mizuno M, Oka N, Kusunoki S, Yamamura T. Selective COX-2 inhibitor celecoxib prevents experimental autoimmune encephalomyelitis through COX-2-independent pathway. *Brain* 2006;129(Pt 8):1984–1992.
76. Kumar JSD, Bai B, Zanderigo F, et al. In Vivo Brain Imaging, Biodistribution, and Radiation Dosimetry Estimation of [<sup>11</sup>C]Celecoxib, a COX-2 PET Ligand, in Nonhuman Primates. *Molecules* 2018;23(8):E1929.
77. Rose JW, Hill KE, Watt HE, Carlson NG. Inflammatory cell expression of cyclooxygenase-2 in the multiple sclerosis lesion. *J Neuroimmunol* 2004;149(1-2):40–49.

78. Wingerchuk DM, Benarroch EE, O'Brien PC, et al. A randomized controlled crossover trial of aspirin for fatigue in multiple sclerosis. *Neurology* 2005;64(7):1267–1269.
79. Mondal S, Jana M, Dasarathi S, Roy A, Pahan K. Aspirin ameliorates experimental autoimmune encephalomyelitis through interleukin-11-mediated protection of regulatory T cells. *Sci Signal* 2018;11(558):eaar8278.
80. Moriguchi K, Miyamoto K, Fukumoto Y, Kusunoki S. 4-Aminopyridine ameliorates relapsing remitting experimental autoimmune encephalomyelitis in SJL/J mice. *J Neuroimmunol* 2018;323:131–135.
81. Arreola-Mora C, Silva-Pereyra J, Fernández T, Paredes-Cruz M, Bertado-Cortés B, Grijalva I. Effects of 4-aminopyridine on attention and executive functions of patients with multiple sclerosis: Randomized, double-blind, placebo-controlled clinical trial. Preliminary report. *Mult Scler Relat Disord* 2019;28:117–124.
82. Savin Z, Lejbkowitz I, Glass-Marmor L, Lavi I, Rosenblum S, Miller A. Effect of Fampridine-PR (prolonged released 4-aminopyridine) on the manual functions of patients with Multiple Sclerosis. *J Neurol Sci* 2016;360:102–109.
83. Rossi S, Studer V, Motta C, et al. Inflammation inhibits GABA transmission in multiple sclerosis. *Mult Scler* 2012;18(11):1633–1635.
84. Kang Y, Rúa SMH, Kaunzner UW, et al. A Multi-Ligand Imaging Study Exploring GABAergic Receptor Expression and Inflammation in Multiple Sclerosis. *Mol Imaging Biol* 2020;22(6):1600–1608.
85. Gilani AA, Dash RP, Jivrajani MN, Thakur SK, Nivsarkar M. Evaluation of GABAergic Transmission Modulation as a Novel Functional Target for Management of Multiple Sclerosis: Exploring Inhibitory Effect of GABA on Glutamate-Mediated Excitotoxicity. *Adv Pharmacol Sci* 2014;2014:632376.
86. Fernández Hurst N, Zanetti SR, Báez NS, Bibolini MJ, Bouzat C, Roth GA. Diazepam treatment reduces inflammatory cells and mediators in the central nervous system of rats with experimental autoimmune encephalomyelitis. *J Neuroimmunol* 2017;313:145–151.
87. Brancati S, Gozzo L, Longo L, Vitale DC, Drago F. Rituximab in Multiple Sclerosis: Are We Ready for Regulatory Approval? *Front Immunol* 2021;12(2600):661882.
88. James ML, Hoehne A, Mayer AT, et al. Imaging B Cells in a Mouse Model of Multiple Sclerosis Using <sup>64</sup>Cu-Rituximab PET. *J Nucl Med* 2017;58(11):1845–1851.
89. Hagens MH, Killestein J, Yaqub MM, et al. Cerebral rituximab uptake in multiple sclerosis: A <sup>89</sup>Zr-immunoPET pilot study. *Mult Scler* 2018;24(4):543–545.
90. MacMillan EL, Schubert JJ, Vavasour IM, et al. Magnetic resonance spectroscopy evidence for declining gliosis in MS patients treated with ocrelizumab versus interferon beta-1a. *Mult Scler J Exp Transl Clin* 2019;5(4):2055217319879952.
91. Bar-Or A, Grove RA, Austin DJ, et al. Subcutaneous ofatumumab in patients with relapsing-remitting multiple sclerosis: The MIRROR study. *Neurology* 2018;90(20):e1805–e1814 [Published correction appears in *Neurology* 2018;91(11):538].
92. Fox E, Lovett-Racke AE, Gormley M, et al. A phase 2 multicenter study of ublituximab, a novel glycoengineered anti-CD20 monoclonal antibody, in patients with relapsing forms of multiple sclerosis. *Mult Scler* 2021;27(3):420–429.
93. Stevens MY, Cropper HC, Lucot KL, et al. Development of a CD19 PET tracer for detecting B cells in a mouse model of multiple sclerosis. *J Neuroinflammation* 2020;17(1):275.
94. Bar-Or A, Pachner A, Menguy-Vacheron F, Kaplan J, Wiendl H. Teriflunomide and its mechanism of action in multiple sclerosis. *Drugs* 2014;74(6):659–674.
95. Prinz C, Starke L, Millward JM, et al. *In vivo* detection of teriflunomide-derived fluorine signal during neuroinflammation using fluorine MR spectroscopy. *Theranostics* 2021;11(6):2490–2504.
96. Einstein O, Feinstein N, Vaknin I, et al. Neural precursors attenuate autoimmune encephalomyelitis by peripheral immunosuppression. *Ann Neurol* 2007;61(3):209–218.
97. Bulte JW, Daldrup-Link HE. Clinical Tracking of Cell Transfer and Cell Transplantation: Trials and Tribulations. *Radiology* 2018;289(3):604–615.
98. Bulte JW, Ben-Hur T, Miller BR, et al. MR microscopy of magnetically labeled neurospheres transplanted into the Lewis EAE rat brain. *Magn Reson Med* 2003;50(1):201–205.
99. Ben-Hur T, van Heeswijk RB, Einstein O, et al. Serial in vivo MR tracking of magnetically labeled neural spheres transplanted in chronic EAE mice. *Magn Reson Med* 2007;57(1):164–171.
100. Muja N, Cohen ME, Zhang J, et al. Neural precursors exhibit distinctly different patterns of cell migration upon transplantation during either the acute or chronic phase of EAE: a serial MR imaging study. *Magn Reson Med* 2011;65(6):1738–1749.
101. Karussis D, Karageorgiou C, Vaknin-Dembinsky A, et al. Safety and immunological effects of mesenchymal stem cell transplantation in patients with multiple sclerosis and amyotrophic lateral sclerosis. *Arch Neurol* 2010;67(10):1187–1194.
102. Gstalder C, Ader I, Cuvillier O. FTY720 (Fingolimod) Inhibits HIF1 and HIF2 Signaling, Promotes Vascular Remodeling, and Chemosensitizes in Renal Cell Carcinoma Animal Model. *Mol Cancer Ther* 2016;15(10):2465–2474.
103. Toh YM, Li TK. Mitoxantrone inhibits HIF-1 $\alpha$  expression in a topoisomerase II-independent pathway. *Clin Cancer Res* 2011;17(15):5026–5037.
104. Bhalla K, Ibrado AM, Tourkina E, et al. High-dose mitoxantrone induces programmed cell death or apoptosis in human myeloid leukemia cells. *Blood* 1993;82(10):3133–3140.
105. Ceronic B, Jacobs BM, Baker D, et al. Cladribine treatment of multiple sclerosis is associated with depletion of memory B cells. *J Neurol* 2018;265(5):1199–1209.
106. Schubert F, Seifert F, Elster C, et al. Serial 1H-MRS in relapsing-remitting multiple sclerosis: effects of interferon- $\beta$  therapy on absolute metabolite concentrations. *MAGMA* 2002;14(3):213–222.
107. Mellergård J, Tisell A, Dahlqvist Leinhard O, et al. Association between change in normal appearing white matter metabolites and intrathecal inflammation in natalizumab-treated multiple sclerosis. *PLoS One* 2012;7(9):e44739.
108. Khan O, Seraji-Bozorgzad N, Bao F, et al. The Relationship Between Brain MR Spectroscopy and Disability in Multiple Sclerosis: 20-Year Data from the U.S. Glatiramer Acetate Extension Study. *J Neuroimaging* 2017;27(1):97–106.
109. Pol S, Sveinsson M, Sudyn M, et al. Teriflunomide's Effect on Glia in Experimental Demyelinating Disease: A Neuroimaging and Histologic Study. *J Neuroimaging* 2019;29(1):52–61.
110. Kreisl WC, Fujita M, Fujimura Y, et al. Comparison of [(11)C]-(R)-PK 11195 and [(11)C]PBR28, two radioligands for translocator protein (18 kDa) in human and monkey: Implications for positron emission tomographic imaging of this inflammation biomarker. *Neuroimage* 2010;49(4):2924–2932.
111. Herranz E, Louapre C, Treaba CA, et al. Profiles of cortical inflammation in multiple sclerosis by <sup>11</sup>C-PBR28 MR-PET and 7 Tesla imaging. *Mult Scler* 2020;26(12):1497–1509.
112. Alam MM, Lee J, Lee SY. Recent Progress in the Development of TSPO PET Ligands for Neuroinflammation Imaging in Neurological Diseases. *Nucl Med Mol Imaging* 2017;51(4):283–296.
113. Singhal T, O'Connor K, Dubey S, et al. 18F-PBR06 Versus 11C-PBR28 PET for Assessing White Matter Translocator Protein Binding in Multiple Sclerosis. *Clin Nucl Med* 2018;43(9):e289–e295.
114. Sridharan S, Raffel J, Nandoskar A, et al. Confirmation of Specific Binding of the 18-kDa Translocator Protein (TSPO) Radioligand [<sup>18</sup>F]GE-180: a Blocking Study Using XBD173 in Multiple Sclerosis Normal Appearing White and Grey Matter. *Mol Imaging Biol* 2019;21(5):935–944.
115. Ravikumar B, Crawford D, Dellovade T, et al. Differential efficacy of the TSPO ligands etifoxine and XBD-173 in two rodent models of Multiple Sclerosis. *Neuropharmacology* 2016;108:229–237.
116. Bunai T, Terada T, Kono S, et al. Neuroinflammation following disease modifying therapy in multiple sclerosis: A pilot positron emission tomography study. *J Neurol Sci* 2018;385:30–33.
117. Ratchford JN, Endres CJ, Hammoud DA, et al. Decreased microglial activation in MS patients treated with glatiramer acetate. *J Neurol* 2012;259(6):1199–1205.
118. Sucksdorff M, Tuisku J, Matilainen M, et al. Natalizumab treatment reduces microglial activation in the white matter of the MS brain. *Neurol Neuroimmunol Neuroinflamm* 2019;6(4):e574.
119. Sucksdorff M, Rissanen E, Tuisku J, et al. Evaluation of the Effect of Fingolimod Treatment on Microglial Activation Using Serial PET Imaging in Multiple Sclerosis. *J Nucl Med* 2017;58(10):1646–1651.
120. Vainio SK, Dickens AM, Tuisku J, et al. Cessation of anti-VLA-4 therapy in a focal rat model of multiple sclerosis causes an increase in neuroinflammation. *EJNMMI Res* 2019;9(1):38.